



Effect of piperine on size, shape and morphology of hydroxyapatite nanoparticles synthesized by the chemical precipitation method

R. Subramanian^{a,b,*}, S. Sathish^b, P. Murugan^b, A. Mohamed Musthafa^c, M. Elango^d

^a Department of Chemistry, Sun Arts and Science College, Thiruvannamalai 606 755, India

^b Department of Chemistry, K.S. Rangasamy College of Arts and Science, Tiruchengode 637 215, India

^c Department of General Studies (Physics Group), Jubail University College (Male Branch), Royal Commission of Jubail, P.O. Box: 10074, Jubail Industrial City, 1961, Saudi Arabia

^d Department of Chemistry, Gnanamani College of Engineering, Namakkal 637 018, India

ARTICLE INFO

Article history:

Received 11 December 2017

Accepted 10 January 2018

Available online 11 January 2018

Keywords:

Piperine

Hydroxyapatite

Nanorods

Organic modifier

Nanostructure

ABSTRACT

The role of piperine, a water insoluble alkaloid compound on the nucleation, crystallinity, size, shape and dispersion of hydroxyapatite (HAp) nanoparticles was investigated. Two different concentrations of piperine were used as an organic modifier. FTIR spectra support the transformation of functional groups. The XRD pattern reveals the crystalline nature of the materials. The TEM images disclose the mechanism of nucleation, formation, shape, size and morphology of HAp nanorods. The addition of the piperine during the synthesis altered the morphology of HAp nanorods. Piperine, as water insoluble alkaloid could affect the morphology of the HAp nanoparticles with agglomeration. These types of well defined and shaped HAp nanorods can be used as a delivery service for drug release and in the field of biomaterial research.

© 2018 Production and hosting by Elsevier B.V. on behalf of King Saud University. This is an open access article under the CC BY-NC-ND license (<http://creativecommons.org/licenses/by-nc-nd/4.0/>).

1. Introduction

Hydroxyapatite (HAp) is a typical calcium phosphate ($\text{Ca}_{10}(\text{PO}_4)_6(\text{OH})_2$) which is a major constituent of both tooth and bone. Due to diversified crystalline structures, HA is a great interest of researchers at present. Their superior biocompatibility and bioactivity lead to fabricate bone grafts in hard tissue engineering. It is used as bone fillers, surface coatings, unloaded scaffolds and dental composites (Bohner, 2001; Ansari et al. 2011). Since its structure is similar to that of bone, attracted the scientific community and engineers towards basic scientific research in biomedical applications (Boskey, 2007; Hench, 1991; Vallet-Regi and Gonzalez-Calbet, 2004; Kalita et al. 2007). Photocatalytic degradation of methyl orange and azo dyes (Shariffuddin et al. 2013; Liu et al. 2016), removal of metals, catalysis in organic synthesis

(Subramanian et al. 2013) and drug delivery (Suresh Kumar et al., 2014). It has received great attention as an excellent candidate for biomedical applications because of its outstanding biocompatibility (Suchanek and Yoshimura, 1998). Hydroxyapatite is one of the major bioceramics, drawn the attention of researcher on various aspects such as synthesis, characterization and its applications (Sopyan et al. 2017). Hydroxyapatite nanoparticles have attracted the researcher due to the vast application in the field of biomedical materials, such as bone fillers, bone tissue engineering scaffolds, soft tissue repairs (Xia et al., 2013; Dorozhkin, 2009; Ji et al., 2012; Bang et al., 2015). HAp nanoparticles used as a potential candidate for controlled drug release from bone implants (Lisa et al. 2016; Rodriguez-Ruiz et al., 2013; Lin et al., 2013). Its usage explored in the field of water treatment and column chromatography for separation of biomolecules, proteins and antibodies as very good biomaterial (Jiang et al. 2012; Hilbrig and Freitag, 2012). The potential application hydroxyapatite nanoparticles evaluated in cell targeting, fluorescence labeling, imaging and diagnosis materials (Kozlova et al., 2012; Chen et al., 2012).

Many organic molecules such as cetyltrimethyl ammonium bromide, triethanolamine, diethanolamine, ethylenediamine tetraacetic acid (EDTA) polyethylene glycol, Tween 20, trisodium citrate, D-sorbitol, citric acid, sodium citrate, sodium dodecylsulphate and sodium dodecylbenzene sulphonates have been employed to control the crystallite size of the hydroxyapatite nanoparticles (Liu et al. 2005; Pramanik et al. 2007; Wang et al.,

* Corresponding author at: Department of Chemistry, Sun Arts and Science College, Thiruvannamalai 606 755, India.

E-mail addresses: subu_m1@yahoo.com (R. Subramanian), sathishselvaraj@gmail.com (S. Sathish), gbusiva@gmail.com (P. Murugan), a.mohamedmusthafa@yahoo.com (A. Mohamed Musthafa), m.elangoche@gmail.com (M. Elango).

Peer review under responsibility of King Saud University.



Production and hosting by Elsevier

2007a,b; Li, 2009; Martins et al. 2008; Chu et al. 2002; Wang et al., 2007a,b). The above stated organic molecules reported to control the nucleation and growth of the HAp nanoparticles during the synthesis. The affinity between the HAp crystals and organic modifiers significantly control the morphology (Berberi et al., 2014).

The relationship between the chelating agent and the crystalline structure of HAp nanoparticles have been studied to understand the role of organic molecules in the synthesis (Rhee and Tanaka, 2000; Vijay Kumar et al. 2016). In addition to organic molecules, polymeric materials like carboxymethyl cellulose also has been used as an organic modifier to produce size controlled HAp nanoparticles (Liu and Lal, 2015). Controlling the agglomeration of particles during the synthesis of HAp is a challenging job and a setback to produce particles with uniform size and shape. Green synthesis of hydroxyapatite, metal substituted synthesis of hydroxyapatite and its applications in various filed have been explored. Green synthesis of silver substituted hydroxyapatite composite as an efficient catalyst for hydration of cyanamides using *Myrica gale* L. extract have been achieved (Momeni et al. 2017). Similarly, silicon-doped hydroxyapatites, nano-rods synthesized by green route have been used as deliver service for antibiotic drug release (Abinaya Sindua et al. 2017). Recently, peptide-tannic acid surface modified hydroxyapatite have synthesized by green method and evaluated as an antifouling agent (Yang et al. 2017). To break down these obstacles, an effort has been taken to control the agglomeration of particles during the synthesis. In addition to the chemical synthesis, green synthesis of HAp is established by means of eco-friendly process. *Aloe vera* extract, leaf extract of *moringa oleifera*, gum-arabic and grape seed extract have been proved as a green chelating agent to synthesis HAp nanoparticles with a well defined shape and size (Klinkaewnarong et al. 2010; Sundrarajan et al. 2015; Sreedhar et al. 2015; Zhou et al., 2012). In plant extract mediated green synthesis, interpretation of the reaction mechanism is not viable because the actual molecule involved in the green synthesis is not identified. It is known that some of the water soluble molecules present in the plant extract may act as reducing agent or chelating agent. Hence, studying the effect of a pure organic molecule on the morphology of HAp is important. The aim of the work is to investigate the role of a water insoluble alkaloid (piperine) on the size, shape, dispersion and morphology of hydroxyapatite nanoparticles.

2. Experimental procedure

Calcium nitrate ($\text{Ca}(\text{NO}_3)_2$), diammonium hydrogen phosphate ($(\text{NH}_4)_2\text{HPO}_4$), ammonium hydroxide, acetone and dichloromethane were purchased from Merck, Mumbai, India. The piperine (Fig. 1) was isolated from the methanolic extract of commercially available black pepper powder and purified using column chromatography according to the literature (Subramanian et al.

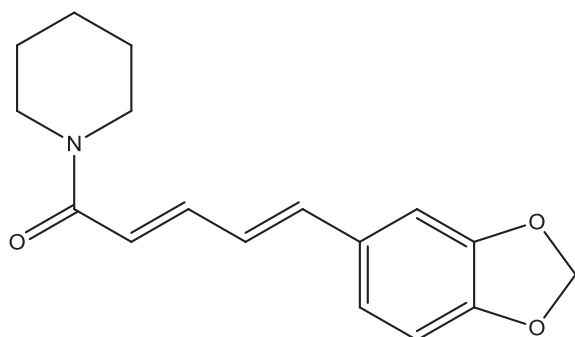


Fig. 1. Structure of piperine.

2016). The purity of the isolated piperine was confirmed by comparing with the commercially available sample. Distilled water was used as the solvent to prepare the solutions.

2.1. Synthesis of hydroxyapatite

Hydroxyapatite was prepared using simple chemical precipitation method (Amiri Roudan et al. 2017). Briefly, 100 ml of (1.0 M) of calcium nitrate and 100 ml of (0.6 M) of diammonium hydrogen phosphate were prepared and the pH of individual solutions was adjusted to 9 by the addition of ammonium hydroxide solution. Both solutions were mixed slowly with constant stirring for an hour at room temperature. Piperine (10 & 20 mg) was dissolved in acetone and added dropwise during the synthesis. The resulted white precipitate was thoroughly washed with double distilled water to remove impurities. The precipitate was dried at 100 °C in hot air oven for 4 h and then used for characterization. The hydroxyapatite synthesized using 10 and 20 mg was named as HAp-10 and HAp-20. A pure hydroxyapatite was also synthesized without piperine for the purpose of comparison.

2.2. Characterization

The function group identification in HAp nanoparticles was studied using an FTIR spectrophotometer (Perkin Elmer Spectrum RXI Spectrometer). The morphology of the prepared samples was studied using Jeol/JEM 2100 Transmission Electron Microscope (TEM), with accelerating voltage 200 kV. The crystallographic structure of the synthesized HA samples was determined by X-ray diffraction using an analytical model X'perPro diffractometer in the range between 20 to 80° at with $\text{Cu K}\alpha$ radiation (1.5406 Å).

3. Results and discussion

The role of piperine in the formation, dispersion and morphological aspects of the HAp nanoparticles was studied. Fig. 2(a–c) shows the FT-IR spectra of the HAp synthesized without and with piperine (10 & 20 mg). The bending vibration and stretching modes (ν_3) noticed at 1286 and 1025 cm^{-1} are corresponds to the phosphate group (PO_4^{3-}). The two broad peaks obtained at 3225 and 3058 cm^{-1} are corresponds to the OH group due to the presence of moisture content (Suresh Kumar et al. 2010). The spectra of all the samples exhibit peak at 1411 cm^{-1} is attributed to the CO_3^{2-} ion. A weak peak noticed at 2097 cm^{-1} in pure HAp is corresponds to ν_3 -asymmetric stretching of carbonate (CO_3^{2-}) ion impurity is

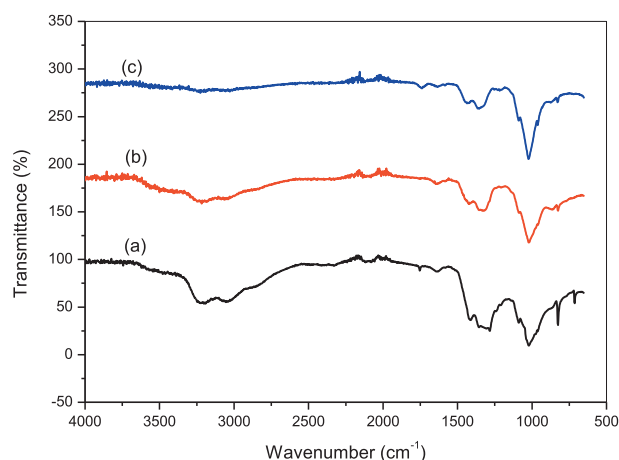


Fig. 2. FTIR spectra of HAp nanoparticles (a) Pure HAp (b) HAp-10 mg piperine (c) HAp-20 mg piperine.

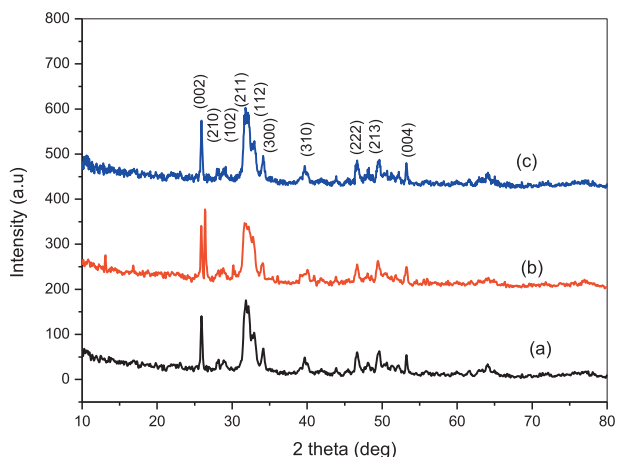


Fig. 3. XRD pattern of HAp nanoparticles (a) Pure HAp (b) HAp-10 mg piperine (c) HAp-20 mg piperine.

disappeared in all the remaining samples. In FT-IR spectra, two sharp peaks appeared at 819 and 718 cm^{-1} are also belongs to ν_2 -vibration of carbonate ion (CO_3^{2-}). Fig. 3(a–c) shows the X-ray

Table 1

Average crystallite size and degree of crystallinity of the pure HAp and HAp synthesized with piperine 10 and 20 mg of piperine.

Sample code	Concentration of piperine (mg)	Average crystallite size (nm)	Degree of Crystallinity
*Pure HAp	0	24.87 ± 02	3.0049
*HAp-10	10	30.80 ± 04	2.7319
*HAp-20	20	29.55 ± 05	2.2334

*Pure HAp: Hydroxyapatite without piperine
 *HAp-10: Hydroxyapatite with 10 mg piperine
 *HAp-20: Hydroxyapatite with 20 mg piperine

diffraction patterns of the HAp synthesized with and without piperine. The XRD patterns of pure HAp and HAp synthesized using 10 and 20 mg of piperine show evidence of diffraction peaks of the standard hydroxyapatite (JCPDS No.9-0432) (Suresh Kumar et al., 2014). The diffraction pattern of the three samples shows no characteristic peaks for calcium hydroxide and calcium phosphates are

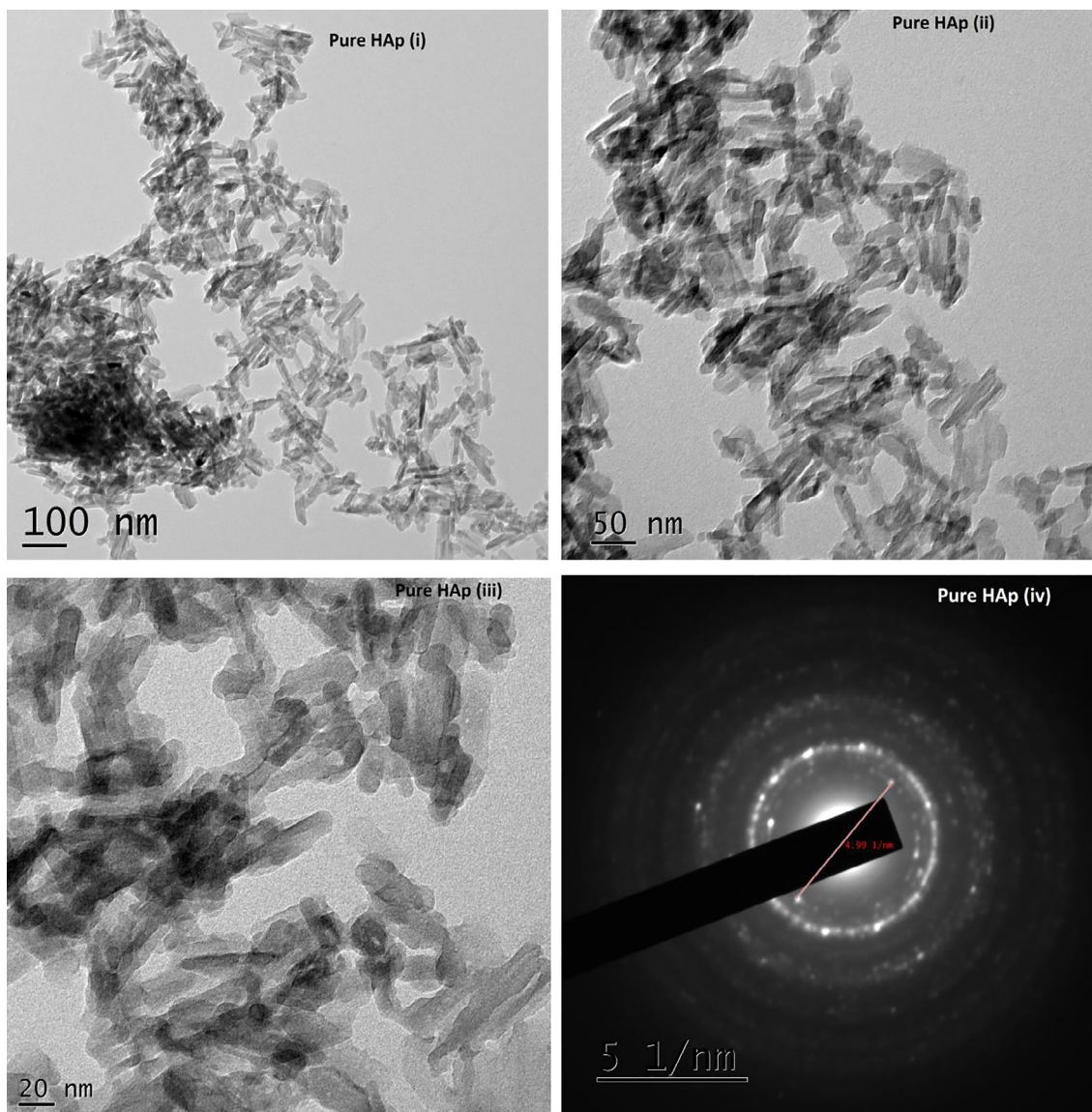


Fig. 4. TEM images of Pure HAp (i–iv) synthesized without piperine.

considered as impurities indicates the purity of the samples. The average crystallite size of the three HAp samples was calculated using Debye–Scherrer's equation is summarized in Table 1. The broad peak observed in the region 30–40° can be recognized to (211), (112), (300) and (202) reflections of HAp. The results of XRD pattern clarify that the crystalline size slightly increased with increasing the concentration of piperine. The changes in the size, shape and dimension of the nanorods are noticed when 10 and 20 mg of the piperine was used. The increases in the width of a particular peak indicate the changes in respective crystal phase. The XRD pattern shows that some changes happened in the crystal plane by the addition of piperine.

The TEM images of pure HAp synthesized without piperine are shown in Fig. 4(i–iv). The HAp sample synthesized without piperine reveals the formation of nanoparticles with agglomeration. The shape of the particles in this image show imperfect and unclear. To understand the role of piperine in the formation of HAp nanoparticles, three different quantities of piperine like 10 and 20 mg were employed. The HAp synthesized using piperine found to be rod-like particles without agglomeration. It exhibits the poor

crystalline nature. The hydroxyapatite nanorods formed are found to be irregular in shape and size with slight agglomeration. Fig. 5(i–iv) show the TEM micrographs of the HAp sample synthesized with 10 mg of piperine. It is observed that nanorods appeared to be slightly improved comparatively good in terms of size and shapes with that of pure HA. Fig. 6(i–iv) exhibit, good appearance and size with evenly distributed nanorods of HAp synthesized using 20 mg of piperine. The shape, size and length of nanorods much improved as compared with that of pure HAp as well as HAp synthesized using 10 mg of piperine. The shapes of the particles are found to be much improved. The size of nanoparticles noticed in TEM micrographs correlates with the XRD pattern of the respective samples. The crystallite size of pure HAp, HAp-10 and HAp-20 obtained from the XRD pattern was ~24.87, 30.80 and 29.55 nm, respectively. It is realized that the size, shape and morphology of HAp crystals formed with two different concentrations of the piperine is appreciably changed. It is also recognized that the HAp nuclei grow into crystallites when the piperine was used as organic modifier. TEM images remarkably revealed the formation of HAp nanoparticles with agglomeration. It is confirmed

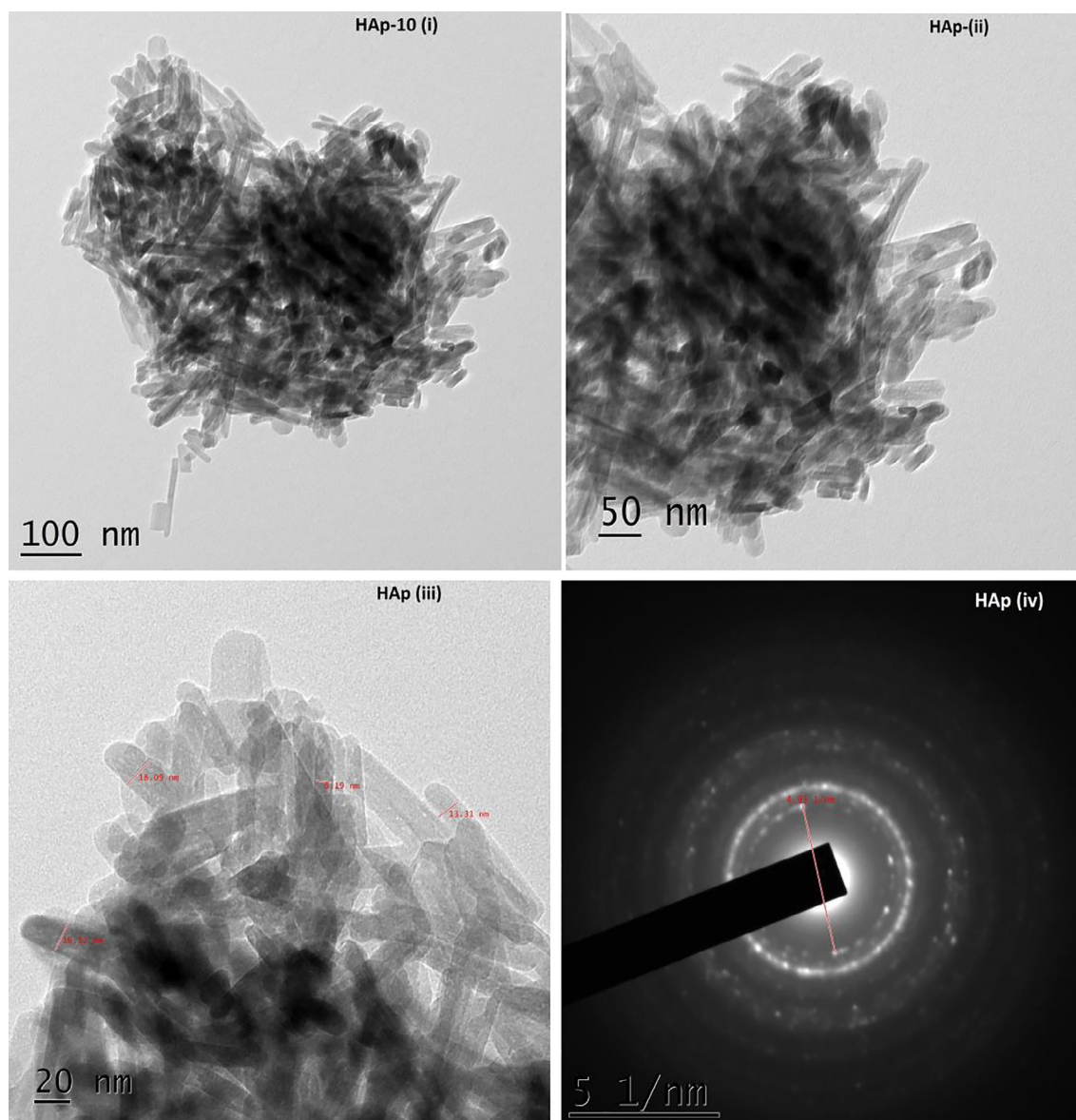


Fig. 5. TEM images of HAp (i–iv) synthesized with 10 mg of piperine.

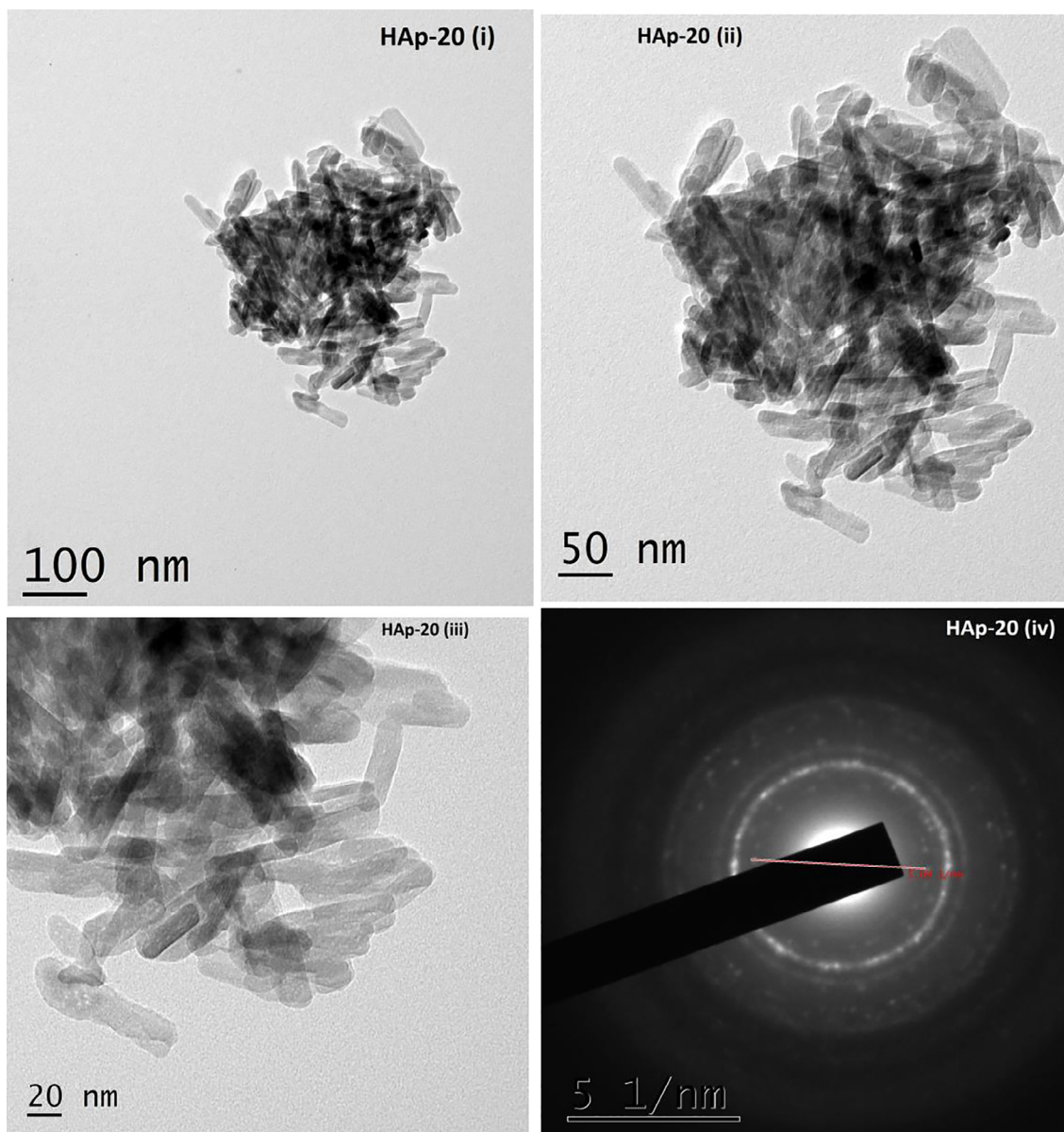


Fig. 6. TEM images of HAp (i–iv) synthesized with 20 mg of piperine.

that the piperine didn't prevent the agglomeration during the synthesis of HAp nanorods. In our case, piperine is absolutely insoluble in water. Hence, it was dissolved in organic solvent, acetone, which is miscible with water and added to the reaction mixture during the synthesis. During the reaction, evaporation of acetone caused the regeneration of piperine. The HAp nanoparticles agglomerated due to the charge of HAp and piperine in the reaction solution. The water insoluble, piperine did not minimize the driving force between the particles, hence the particles could not be freely dispersed. Here, piperine acted as a modifier in terms of shape and morphology of the particles without controlling the driving force between the particles. The size of HAp nanoparticles synthesized with and without piperine is almost similar. It is understood that piperine acts as a modifier by means of controlling the shape of the particles and not the size due to its insoluble nature in water. In our findings, we highlighted that the formation of lengthy HAp nanorods with aggregation of crystals in particular at two concentrations (10 & 20 mg). Evidently, piperine effects some changes in the size, shape and morphology of the particles when it was used

as an organic modifier. Some of the organic modifiers such as citric acid (Chu et al. 2002), EDTA (Wang et al., 2007a,b) and trisodium citrates (Rhee and Tanaka, 2000; Yang et al. 2013) are proven to control the size, shape and morphology of the HAp particles during the synthesis. It is known that the above stated organic compounds are freely soluble in water. The aqueous solution of organic compound and aqueous solution of calcium ammonium salt are easily miscible together. But in case of piperine, the molecule itself aggregates when the organic solvent is evaporated during the synthesis. HAp nanorods synthesized without piperine seem to be aggregated together seriously without perfect shapes. The average diameters and the average lengths of the HAp nanorods increased with increasing concentration of piperine. The presence of piperine (10 & 20 mg) was helpful in the formation of well defined, shaped HAp nanorods as compared with that of pure HAp. It can be recommended that piperine as an organic modifier has slight effects on the sizes of the particles and significantly altered the shape of the particles. The interaction between the piperine and HAp crystallite consequently produces HAp nanorods with long lengths as

compared with pure HAP. Though many water soluble organic compounds and aqueous extract of many plants have been used as a green chelating agent to modify the surface of the hydroxyapatite nanoparticles. Such nanoparticles also produced in various fascinating shapes and evaluated for various applications. First time we used piperine, a water insoluble compound to produce HAP nanorods. This is the first report added in the field of organic modifier to produce HAP nano rods with well defined shapes.

4. Conclusion

Hydroxyapatite nanorods were synthesized with and without piperine by the chemical precipitation method. Piperine played a vital role to initiate the nucleation of particles during the synthesis. It is proved that piperine, initiate the nucleation and control the shape of the particles with agglomeration. The pure HAP nanocrystals synthesized without piperine exhibit aggregation with imperfection in the shape and size. Piperine tainted the surface morphology of HAP nano structures. The TEM images clearly differentiate the shape of HAP synthesized with and without piperine. The results of this work showed that piperine improve the morphology, especially the shape of HAP nanoparticles. Piperine as an organic molecule could control the morphology of the particles during the synthesis to some extent. Since it is insoluble in water, it could not prohibit the agglomeration of particles. First time, we disclose the fact that the water insoluble organic molecule cannot control the agglomeration, but it modifies the shape and size of the nanoparticles. Hence, this type of specific shaped HAP nanorods can be utilized for drug delivery and other material applications.

Acknowledgments

The authors express their sincere thanks to UGC, Hyderabad, New Delhi, India (Project Ref. No. MRP-5397/14-SERO/UGC) for financial support. The authors also thank Karunya University (Coimbatore), St Joseph College (Trichy) and SAIF, Cochin University of Science and Technology, Cochin for providing FTIR, XRD and TEM facilities for characterization.

References

- Amiri Roudan, M., Ramesh, S., Niakanb, A., Wonga, Y.H., Akhtari Zavareha, M., Chandran, Hari, Teng, Wd, Lwin, L., Sutharsinif, U., 2017. Thermal phase stability and properties of hydroxyapatite derived from biowaste eggshells. *J. Ceram. Proc. Res.* 18, 69–72.
- Abinaya Sindua, P., Kolanthai, E., Suganthi, R.V., Thanigai, K., Manikandan, A.E., Catalani, L.H., Narayana Kalkura, S., 2017. Green synthesis of Si-incorporated hydroxyapatite using sodium metasilicate as silicon precursor and in vitro antibiotic release studies. *J. Photochem. Photobiol. B: Biol.* 175, 163–172.
- Ansari, M., Naghib, S.M., Moztaizadeh, F., Salati, A., 2011. Synthesis and characterization of hydroxyapatite-calcium hydroxide for dental composites. *Ceram. Silik.* 55, 123–126.
- Bang, L.T., Ramesh, S., Purbolaksono, J., Long, B.D., Chandran, Hari, Ramesh, S., Othman, R., 2015. Development of a bone substitute material based on alpha-tricalcium phosphate scaffold coated with carbonate apatite/poly-epsilon-caprolactone. *Biomed. Mater.* 10, 045011.
- Berberi, A., Samarani, A., Nader, N., Noujeim, Z., Dagher, M., Kanj, W., Mearawi, R., Saleme, Z., Badran, B., 2014. Physicochemical characteristics of bone substitutes used in oral surgery in comparison to autogenous bone. *BioMed. Res. Int.* 2014, 1–9.
- Bohner, M., 2001. Physical and chemical aspects of calcium phosphates used in spinal surgery. *Eur. Spine J.* 10, S114–S121.
- Boskey, A.L., 2007. Mineralization of bones and teeth. *Elements* 3, 387–393.
- Chu, C.L., Lin, P.H., Dong, Y.S., Guo, D.Y., 2002. Influences of citric acid as a chelating reagent on the characteristics of nanophase hydroxyapatite powders fabricated by a sol-gel method. *J. Mater. Sci. Lett.* 21, 1793–1795.
- Chen, F., Huang, P., Zhu, Y.J., Wu, J., Cui, D.X., 2012. Multifunctional Eu³⁺/Gd³⁺ dual-doped calcium phosphate vesicle-like nanospheres for sustained drug release and imaging. *Biomaterials* 33, 6447–6455.
- Dorozhkin, S.V., 2009. Calcium orthophosphates in nature. *Biol. Med. Mater.* 2, 399–498.
- Hench, L.L., 1991. Bioceramics: From Concept to Clinic. *J. Am. Ceram. Soc.* 74, 1487.
- Hilbrig, F., Freitag, R., 2012. Isolation and purification of recombinant proteins, antibodies and plasmid DNA with hydroxyapatite chromatography. *Biotechnol. J.* 7, 90–102.
- Jiang, S.D., Yao, Q.Z., Zhou, G.T., Fu, S.Q., 2012. Fabrication of hydroxyapatite hierarchical hollow microspheres and potential application in water treatment. *J. Phys. Chem. C* 116, 4484–4492.
- Ji, D.-Y., Kuo, T.-F., Wu, H.-D., Yang, J.-C., Lee, S.-Y., 2012. A novel injectable chitosan/polyglutamate polyelectrolyte complex hydrogel with hydroxyapatite for soft-tissue augmentation. *Carbohydr. Polym.* 89, 1123–1130.
- Kalita, S.J., Bhardwaj, A., Bhatt, H.A., 2007. Nanocrystalline calcium phosphate ceramics in biomedical engineering. *Mater. Sci. Eng. C* 27, 441–449.
- Klinkaewnarong, J., Swatsitang, E., Masingboon, C., Seraphin, S., Maensiri, S., 2010. Synthesis and characterization of nanocrystalline HAP powders prepared by using aloe vera plant extracted solution. *Cur. Appl. Phys.* 10, 521–525.
- Kozlova, D., Chernousova, S., Knuschke, T., Buer, J., Westendorf, A.M., Epple, M., 2012. Cell targeting by antibody-functionalized calcium phosphate nanoparticles. *J. Mater. Chem.* 22, 396–404.
- Lisa, C., Nikolaos, B., Dimitrios, F., Ioanna, K., Marta, R., 2016. Synthesis of carbon nanotubes loaded hydroxyapatite: potential for controlled drug release from bone implants. *J. Adv. Ceram.* 5, 232–243.
- Lin, K., Liu, P., Wei, L., Zou, Z., Zhang, W., Qian, Y., et al., 2013. Strontium substituted hydroxyapatite porous microspheres: surfactant-free hydrothermal synthesis, enhanced biological response and sustained drug release. *Chem. Eng. J.* 222, 49–59.
- Li, C., 2009. Crystalline behaviors of hydroxyapatite in the neutralized reaction with different citrate additions. *Powder Technol.* 192, 1–5.
- Liu, W., Qian, G., Zhang, B., Liu, L., Liu, H., 2016. Facile synthesis of spherical nano hydroxyapatite and its application in photocatalytic degradation of methyl orange dye under UV irradiation. *Mater. Lett.* 178, 15–17.
- Liu, J., Li, K., Wang, H., Zhu, M., Xu, H., Yan, H., 2005. Self-assembly of hydroxyapatite nanostructures by microwave irradiation. *Nanotechnology* 16, 82–87.
- Liu, R., Lal, R., 2015. Effects of molecular weight and concentration of carboxymethyl cellulose on morphology of hydroxyapatite nanoparticles as prepared with one-step wet chemical method. *Front. Environ. Sci. Eng.* 9, 804–812.
- Martins, M.A., Santos, C., Almeida, M.M., Costa, M.E.V., 2008. Hydroxyapatite micro and nanoparticles: Nucleation and growth mechanisms in the presence of citrate species. *J. Colloid Interface Sci.* 318, 210–216.
- Momeni, S.S., Nasrollahzadeh, M., Rustaiyan, A., 2017. Biosynthesis and application of Ag/bone nanocomposite for the hydration of cyanamides in *Myrica gale L.* extract as a green solvent. *J. Colloid Interface Sci.* 499, 93–101.
- Pramanik, N., Tarafdar, A., Pramanik, P., 2007. Capping agent-assisted synthesis of nanosized hydroxyapatite: comparative studies of their physicochemical properties. *J. Mater. Process Technol.* 184, 131–138.
- Rhee, S.H., Tanaka, J., 2000. Hydroxyapatite formation on cellulose cloth induced by citric acid. *J. Mater. Sci. Mater. Med.* 11, 449–452.
- Rodriguez-Ruiz, I., Delgado-Lopez, J.M., Duran-Olivencia, M.A., Iafisco, M., Tampieri, A., Colangelo, D., et al., 2013. pH-Responsive delivery of doxorubicin from citrate-apatite nanocrystals with tailored carbonate content. *Langmuir* 29, 8213–8221.
- Shariffuddin, J.H., Ian Jones, M.D., Patterson, A., 2013. Greener photocatalysts: Hydroxyapatite derived from waste mussel shells for the photocatalytic degradation of a model azo dye wastewater. *Chem. Eng. Res. Design* 91, 1693–1704.
- Sreedhar, B., Keerthi Devi, D., Sai Neetha, A., Pavan Kumar, V., Chary, K.V.R., 2015. Green synthesis of gum-acacia assisted gold-hydroxyapatite nanostructures: Characterization and catalytic activity. *Mater. Chem. Phys.* 153, 23–31.
- Subramanian, R., Noorul Ameen, J., Subbramanyan, P., Raj, V., 2016. Double bypasses Soxhlet apparatus extraction of piperine from *piper nigrum*. *Arab. J. Chem.* 9, S537–S540.
- Sundrarajan, M., Jegatheeswaran, S., Selvam, S., Sanjeevi, N., Balaji, M., 2015. The ionic liquid assisted green synthesis of hydroxyapatite nanoplates by *Moringa oleifera* flower extract: A biomimetic approach. *Mater. Design* 88, 1183–1190.
- Suresh Kumar, G., Girija, E.K., Thamizhavel, A., Yokogawa, Y., Narayana Kalkura, S., 2010. Synthesis and characterization of bioactive hydroxyapatite-calcite nanocomposite for biomedical applications. *J. Colloid Interface Sci.* 349, 56–62.
- Subramanian, M., Vanangamudi, G., Thirunarayanan, G., 2013. Hydroxyapatite catalyzed aldol condensation: synthesis, spectral linearity, antimicrobial and insect antifeedant activities of some 2, 5-dimethyl-3-furyl chalcones. *Spectrochim. Acta Part A: Mol. Biomol. Spectrosc.* 110, 116–123.
- Suresh Kumar, G., Govindan, R., Girija, E.K., 2014. In situ synthesis, characterization and in vitro studies of ciprofloxacin loaded hydroxyapatite nanoparticles for the treatment of osteomyelitis. *J. Mater. Chem. B* 2, 5052–5060.
- Suchanek, W., Yoshimura, M., 1998. Processing and properties of hydroxyapatite-based biomaterials for use as hard tissue replacement implants. *J. Mater. Res.* 13, 94–117.
- Sopyan, I., Pusparini, E., Ramesh, S., Tanc, C.Y., Ching, Y.C., Wong, Y.H., Zainal Abidin, N.I., Chandrand, Hari, Ramesh, S., Bang, L.T., 2017. Influence of sodium on the properties of sol-gel derived hydroxyapatite powder and porous scaffolds. *Ceram. Int.* 43, 12263–12269.
- Vallet-Regi, M., Gonzalez-Calbet, J.M., 2004. Calcium phosphates as substitution of bone tissues. *Prog. Solid State Chem.* 32, 1–31.
- Vijay Kumar, M., Birendra, N.B., Devendra, K., Shyam, B.R., Parkashb, Om, 2016. Effect of chelating agent at different pH on spectroscopic and structural properties of microwave derived hydroxyapatite nanoparticles: a bone mimetic material. *New J. Chem.* 40, 5432–5441.

- Wang, A., Yin, H., Liu, D., Wu, H., Wada, Y., Ren, M., Xu, Y., Jiang, T., Cheng, X., 2007a. Effects of organic modifiers on the size-controlled synthesis of hydroxyapatite nanorods. *Appl. Surf. Sci.* 253, 3311–3316.
- Wang, A., Liu, D., Yin, H., Wu, H., Wada, Y., Ren, M., Jiang, T., Cheng, X., Xu, Y., 2007b. Size-controlled synthesis of hydroxyapatite nanorods by chemical precipitation in the presence of organic modifiers. *Mater. Sci. Eng. C* 27, 865–869.
- Xia, L., Lin, K., Jiang, X., Xu, Y., Zhang, M., Chang, J., et al., 2013. Enhanced osteogenesis through nano-structured surface design of macroporous hydroxyapatite bioceramic scaffolds via activation of ERK and p38 MAPK signaling pathways. *J. Mater. Chem. B* 1, 5403–5416.
- Yang, C.C., Lin, C.C., Liao, J.W., Yen, S.K., 2013. Vancomycin–chitosan composite deposited on post porous hydroxyapatite coated Ti₆Al₄V implant for drug controlled release. *Mater. Sci. Eng. C* 33, 2203–2212.
- Yang, X., Huang, P., Wang, H., Cai, S., Liao, Y., Mo, Z., Xu, X., Ding, C., Zhao, C., Li, J., 2017. Antibacterial and anti-biofouling coating on hydroxyapatite surface based on peptide-modified tannic acid. *Colloids Surfaces B* 160, 136–143.
- Zhou, R., Si, S., Zhang, Q., 2012. Water-dispersible hydroxyapatite nanoparticles synthesized in aqueous solution containing grape seed extract. *Appl. Surf. Sci.* 258, 3578–3583.